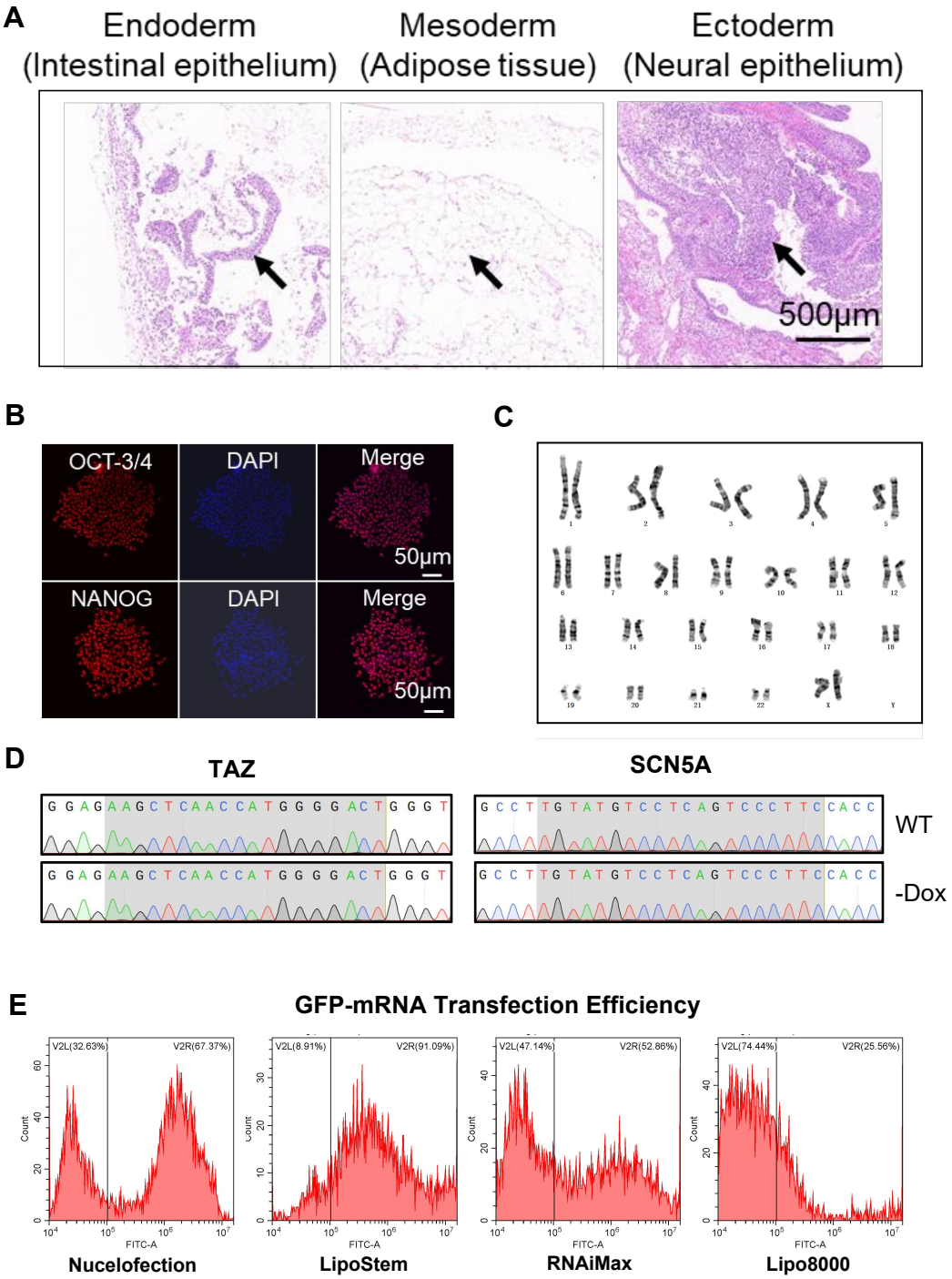

Figure S1. Characterization of hPSCs-iCas9

(A) Hematoxylin and eosin (HE) staining of the teratomas derived from H9-iCas9 cells. Arrows indicate the presence of endoderm (Intestinal epithelium), mesoderm (adipose), and ectoderm (neural epithelium). Scale bar=500 μm. (B) IFA staining for pluripotency markers OCT3/4 and NANOG in H9-iCas9. Cells were counterstained with DAPI to visualize nuclei. Scale bar=50 μm. (C) Karyotype analysis of H9-iCas9 line. (D) Sanger sequencing to detect the potential nuclease leakage. H9-iCas9 cells nucleofected with sgRNAs targeting the TAZ or SCN5A gene without Dox addition showed no visible edits in the suspected editing regions (areas in shadow) compared to Wild-type (WT). (E) Flow cytometry analysis of GFP-positive cells following GFP-mRNA transfection using different reagents. $8x10^5$ cells were transfected with 5 μg mRNA.

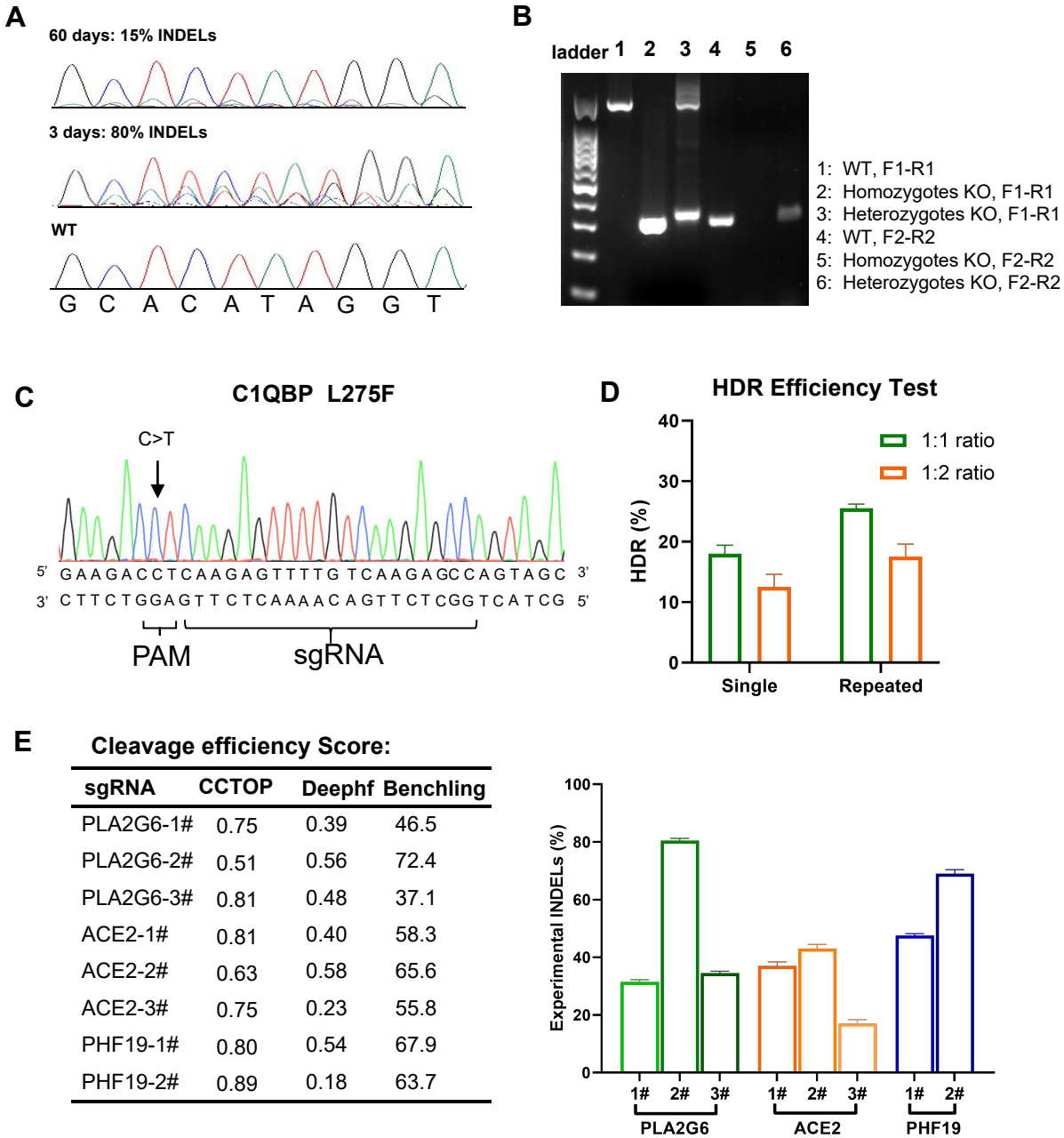

sgRNA	CCTOP	Deephf	Benchling
PLA2G6-1#	0.75	0.39	46.5
PLA2G6-2#	0.51	0.56	72.4
PLA2G6-3#	0.81	0.48	37.1
ACE2-1#	0.81	0.40	58.3
ACE2-2#	0.63	0.58	65.6
ACE2-3#	0.75	0.23	55.8
PHF19-1#	0.80	0.54	67.9
PHF19-2#	0.89	0.18	63.7

Figure S2. Gene editing performance of optimized hPSCs-iCas9

(A) Sanger sequencing chromatograms showing a notable reduction in INDELs incorporation from 3 to 60 days. (B) Representative gel electrophoresis of PCR products of paired sgRNA-mediated gene knockouts. Lane 1/2/3 depicts amplification with external primers (F1, R1), while lane 4/5/6 depicts amplification with internal primers (F2, R2). Lane 1/4 represents Wild-type, lane 2/5 represents homozygous knockout, and lane 3/6 represents heterozygous knockout. Full-length gels are presented in Figure S5. (C) Schematic diagram of the C1QBP-L275F (CTC>TTC) mutation and the sgRNA design for HDR. Following HDR, the mutation replaces the wild-type nucleic acid, thereby removing the PAM. (D) Optimization of sgRNA-to-ssODN ratio to enhance HDR efficiency. The total nucleic acid for nucleofection was fixed at 5 μg. Data represent the average of two replicates. (E) Validation of cleavage efficiency scores against the actual edits. Left: Cleavage efficiency predicted by three different scoring algorithms. Right: Experimental INDELs efficiency of sgRNAs targeting various gens determined in H9-iCas9. Data are shown as mean ± SD, n=2.

A

B

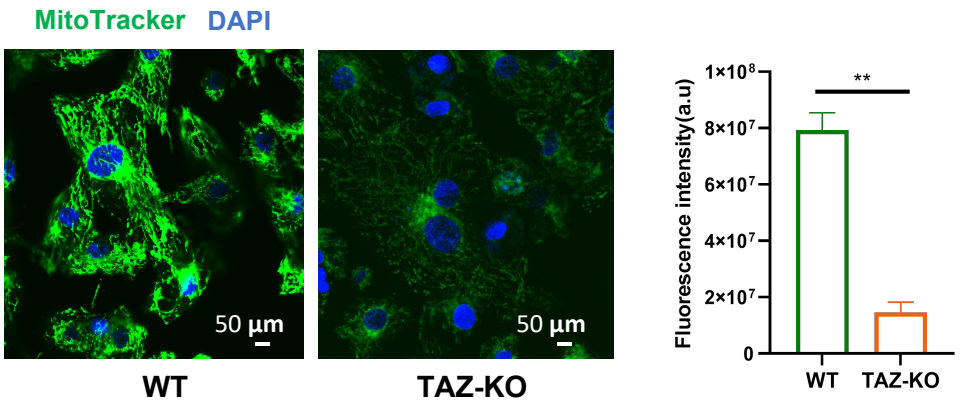

Figure S3. (A) ICE analysis of Sanger sequencing chromatograms for gene knockout on each exon. (B) Significantly reduced mitochondrial potential and activity of TAZ-KO cardiomyocytes. hPSCs-CMs were stained with MitoTracker Green and imaged with a confocal microscope. Left: Representative images, scale bar = 50 μm. Right: Quantitative analysis of mitochondrial staining intensity. Two-tailed *t*-test.

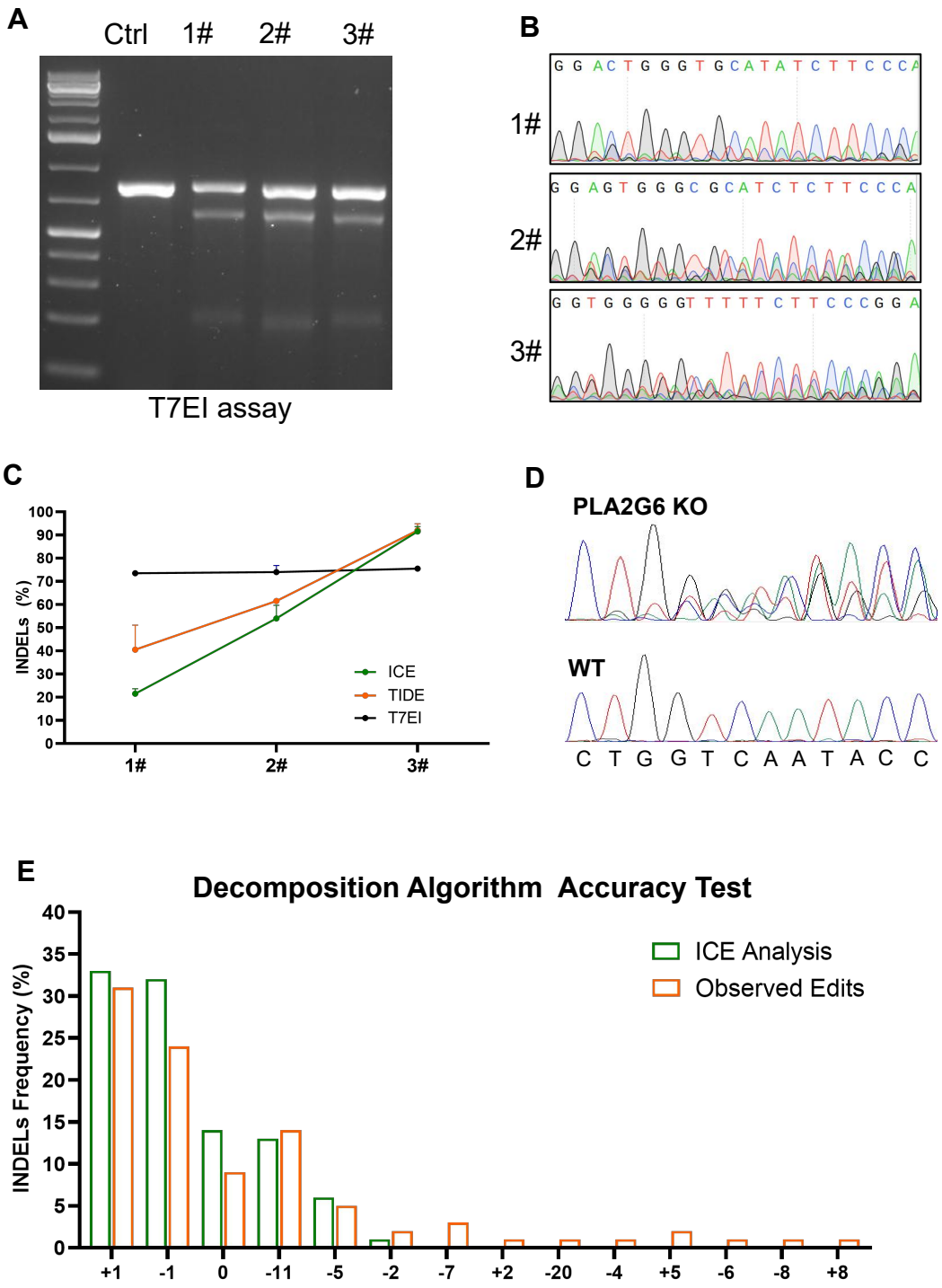

Figure S4. Validation of ICE analysis accuracy

(A) Representative gel electrophoresis image of PCR products from three edited cells pools (1# to 3#) digested by of 7TE1. Full-length gels are presented in Figure S5. (B) Sanger sequencing chromatograms of edited cells pools. (C) INDELs efficiency analyzed 7TE1, TIDE and ICE. n=3. (D) Sanger sequencing chromatograms of the edited cells pool nucleofected with sgRNA targeting PLA2G6. (E) Comparison of actual edits obtained from single-sorted cells with ICE-analyzed Sanger sequencing chromatograms.

Fig. 2B

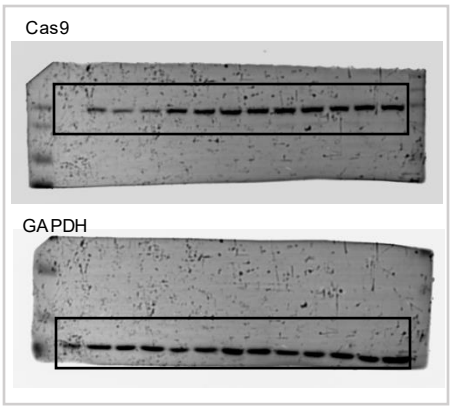

Fig. 2D

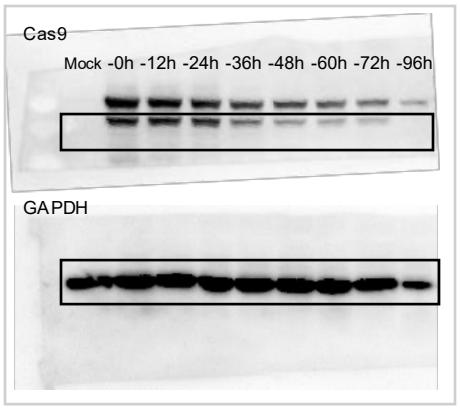

Fig. 6F

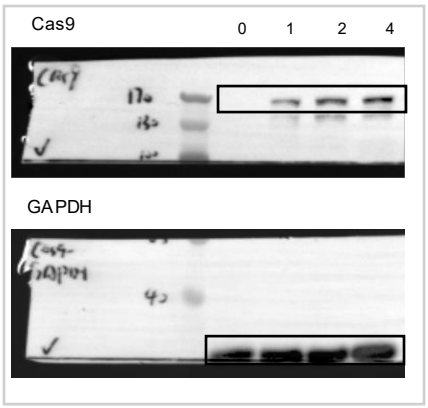

Fig. 5D

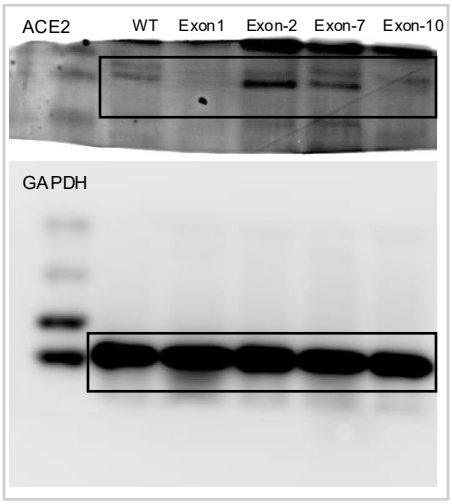

Fig. 5F

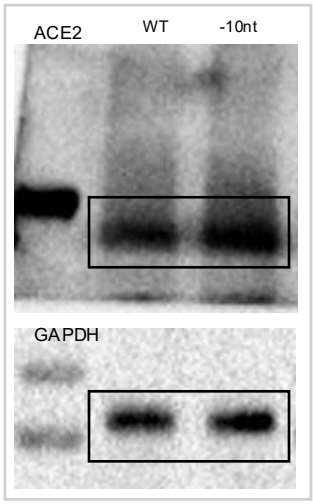

Fig. S2B

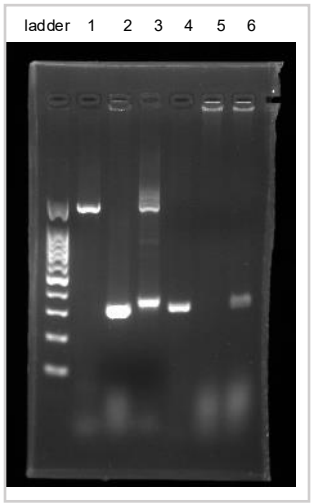

Fig. S4A

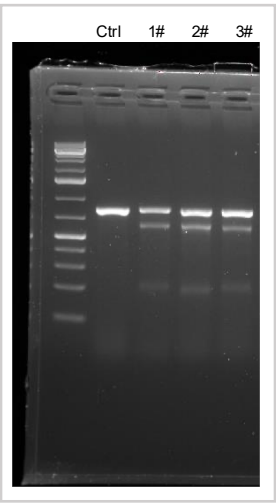

Figure S5. The image of full-length blots/gels.

The images in figures are cropped according to the black box.